Research Square

Preprints are preliminary reports that have not undergone peer review.
They should not be considered conclusive, used to inform clinical practice,
or referenced by the media as validated information.

Reversible C–C Bond Formation Using Palladium Catalysis

Austin Marchese
University of Toronto https://orcid.org/0000-0002-3090-2748
Bijan Mirabi
University of Toronto https://orcid.org/0000-0002-4852-3439
Colton Johnson
University of Toronto https://orcid.org/0000-0002-0905-1248
Mark Lautens (mark.lautens@utoronto.ca)
University of Toronto https://orcid.org/0000-0002-0179-2914

Article

Keywords: C-C bonds, reactions, metal-catalyzed reactions

Posted Date: May 13th, 2021

DOI: https://doi.org/10.21203/rs.3.rs-426770/v1

License: This work is licensed under a Creative Commons Attribution 4.0 International License.
Read Full License

Version of Record: A version of this preprint was published at Nature Chemistry on March 17th, 2022. See the published version at https://doi.org/10.1038/s41557-022-00898-0.

Reversible C–C Bond Formation Using Palladium Catalysis

Authors: Austin D. Marchese[1†], Bijan Mirabi[1†], Colton E. Johnson[1], Mark Lautens[1]*

Affiliations:

[1]Department of Chemistry, Davenport Chemical Laboratories, University of Toronto, Toronto, Ontario M5S 3H6, Canada.

*Correspondence to: Department of Chemistry, Davenport Chemical Laboratories, University of Toronto, Toronto, Ontario M5S 3H6, Canada; orcid.org/0000-0002-0179- 2914; Email: mark.lautens@utoronto.ca.

†These authors contributed equally.

Abstract: A widely appreciated principle is that all reactions are fundamentally reversible. Observing reversible transition metal-catalyzed reactions, particularly those that include the cleavage of C–C bonds, are more challenging. The development of the palladium- and nickel-catalyzed carboiodination reactions afforded access to the *syn*- and *anti*-diastereomers of the iodo-dihydroisoquinolone products. Using these substrates, an extensive study investigating the catalytic reversibility of the C–C bond formation using a different palladium catalyst was undertaken. A combination of experimental and computational studies led to the discovery of a variety of new methodologies and concepts key to understanding the process of reversible C–C bond formations.

Main Text: A fundamental tenant of chemical reactivity is that reactions are reversible. Classic organic transformations, illustrated by the Diels-Alder reaction[1–3] and the aldol condensation,[4–6] have been thoroughly studied in both the forward and reverse directions. Transition metal-catalyzed processes, such as β-hydride elimination, or its microscopic reverse hydrometallation process, have been widely studied.[7–10] A thorough investigation of these fundamental steps where a C–H bond is made or broken has been enabled, in part, by easily designed kinetic isotope experiments involving deuterated substrates.[7–10] Analogous transformations involving carbon have garnered less attention due to their increased rarity as the systems to interrogate this process difficult to design. Migratory insertion involving C–C bond formation is a key step in many transition metal-catalyzed transformations, including the Mizoroki-Heck reaction. Examples of the microscopic reverse process, β-carbon elimination, have been reported in the literature;[11–15] however, most have been observed when key structural elements are present (Scheme 1). The most prevalent β-carbon eliminations are driven by release of ring strain.[16–20] The most common examples of this are when cyclic alcohols are used to form metal homoenolate nucleophiles (Scheme 1a).[16] The relief of steric strain via a β-carbon elimination, as seen in the Catellani reaction, rely on the build-up of increasing steric encumbrance during the course of the reaction (Scheme 1b).[17,21,22] Other strategies to enable β-carbon eliminations rely on the formation of a strong π-bond (Scheme 1c).[17,19,23–29] These biased systems make it difficult to study the effects of different parameters on the β-carbon elimination process, and thus an unbiased system would not only be conceptually novel, but allow for the examination of other parameters on reversible C–C bond cleavage. In this work, we have identified a substrate that enables insight into the β-carbon elimination, a concept that to our knowledge has not been explored. Furthermore, isotopically

enriched heavy atoms are not required. A reversible process has been found that offers an optimal starting point for further studies in this important reaction manifold (Scheme 1d).

In 2010, we identified reversible oxidative addition into C–Br bonds as part of a synthetically useful catalytic cycle[30] and utilized this process in the development of a carbohalogenation reaction catalyzed by palladium.[31,32] The carbohalogenation reaction enables the transfer of an aryl-iodide across a tethered π-bond with formation of a new C–I bond using a Pd(0) precatalyst and sterically hindered phosphine ligands. This cycloisomerization reaction proved to be quite general as both the palladium- and nickel-catalyzed carboiodination provided access to a variety of structurally diverse compounds.[32,33,42–44,34–41] In particular, in 2014 we reported the palladium-catalyzed carboiodination reaction to generate *syn* iodo-dihydroisoquinolones[37] and in 2019 reported the nickel catalyzed variant which gave access to the corresponding *anti*-iodo-dihydroisoquinolones.[41] With access to both the *anti*- and *syn*- diastereomers of the iodinated compounds, we had an ideal opportunity to investigate the reversibility of the carbohalogenation process.

By subjecting the *anti*-diastereomer formed in the nickel-catalyzed carboiodination reaction to a palladium catalyst incapable of performing the C–I reductive elimination,[45] we identified a palladium-catalyzed β-carbon elimination, cleaving the unstrained 6-membered ring containing an all-carbon quaternary stereocenter, followed by reformation of the same C–C bond with the stereochemistry observed in the palladium-catalyzed process. Herein, we describe our studies that shed light on mechanism of this reaction involving a catalytically reversible β-carbon elimination and outline new stereoelectronic factors for this β-carbon elimination process supported by experimental and computational evidence. In addition, we developed an efficient catalytic strategy for the diastereoconvergent formation of indenodihydroisoquinolones via a palladium-catalyzed net epimerization arising from reversible C–C bond formation followed by C–H activation. The products could be obtained as a single diastereomer in up to 95% yield when starting from a 1:1 mixture of diastereomeric starting materials and 94% yield when starting with only the *anti*-diastereomer.

The *anti*-diastereomer ***anti*-1a**, arising from a nickel-catalyzed carboiodination reaction, was subjected to $Pd(PPh_3)_4$ (30 mol%), K_2CO_3 (4 equiv.) in toluene (0.07 M) at 120 °C for 24 h, yielding the *syn* tetracyclic product in 45% yield (Scheme 2a), with the majority of the mass balance being the protodemetalated product, **3a**. X-ray crystallography unambiguously confirmed that the stereochemistry of the quaternary center was opposite to that of the starting material. When subjecting ***lin*-1a** to the same reaction conditions**,** the product was obtained in a slightly increased yield of 55% when compared to ***anti*-1a**, accompanied by a reduced yield of the protodemetalated side product. When employing ***syn*-1a**; the product generated from a palladium-catalyzed carboiodination reaction, the same syn-product was obtained in the highest yield of 79%, with <10% of the protodemetalated intermediate.

Scheme 1. Classic Examples of β-carbon elimination and Our Work

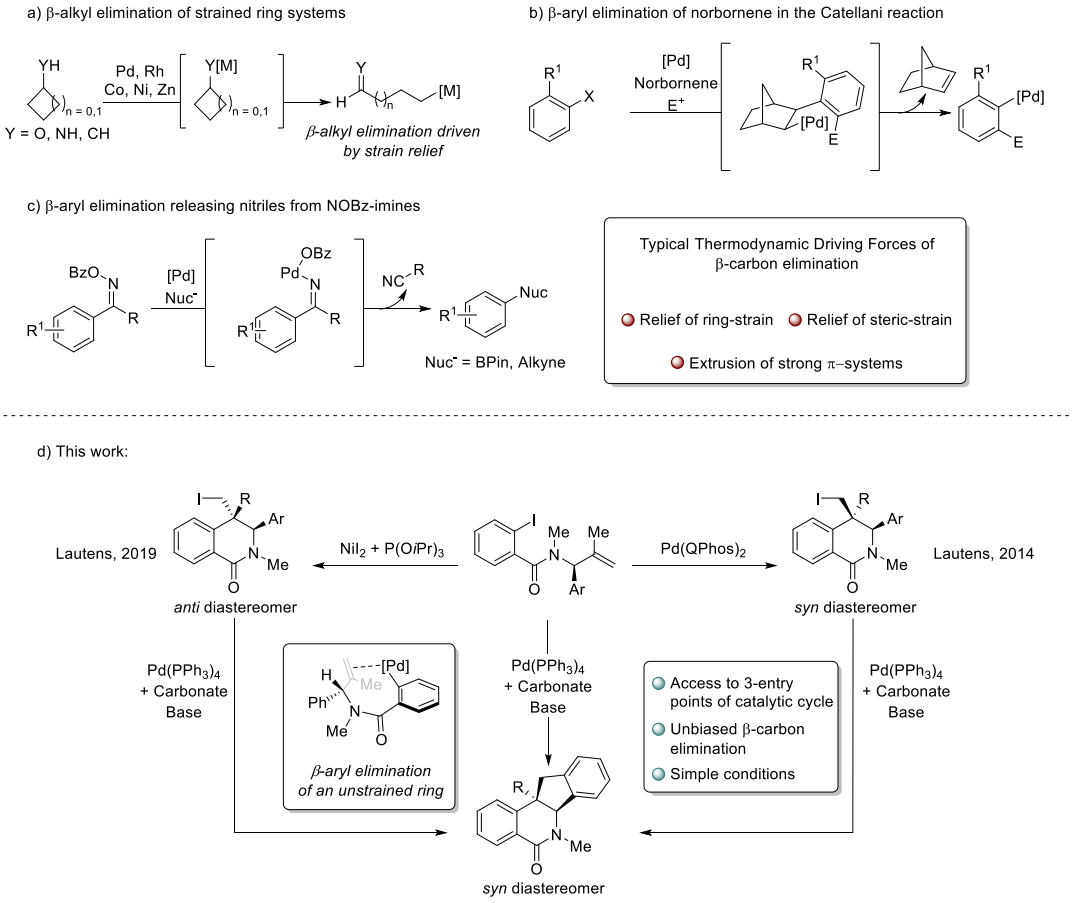

These results are in agreement with the proposed β-carbon elimination pathway (Scheme 2d), as a higher yield of product was observed when starting from a later point along the proposed catalytic cycle.

We speculated that the transformation initiates via an oxidative addition of the palladium(0) catalyst to the neopentyl iodide, followed by a β-carbon elimination, which yields an aryl palladium(II) intermediate. We had previously documented that this Ar–Pd(II)–X species has a high propensity to undergo cyclization with *syn*-diastereoselectivity.[37,46,47] Following the β-carbon elimination, the resulting palladium(II) complex could isomerize from one face of the olefin to the other through a dissociative mechanism, which allows for the subsequent migratory insertion process. This sequence results in the cleavage and reformation of an all-carbon quaternary center, however with opposite diastereoselectivity. The resulting neopentyl palladium species is poised to undergo a C–H activation and reductive elimination of the pendant aromatic ring, generating the tetracyclic indenodihydroisoquinolone structure. We speculated that the *anti*-diastereomer would not undergo C–H activation of the pendant aromatic ring due to the resulting strain of the *anti* 6-5 fused ring system and by employing a ligand (PPh_3) that has been previously shown to be incapable of C–I reductive elimination with palladium, we could study a β-carbon elimination process.

Scheme 2. Initial Results and Proposed Mechanism

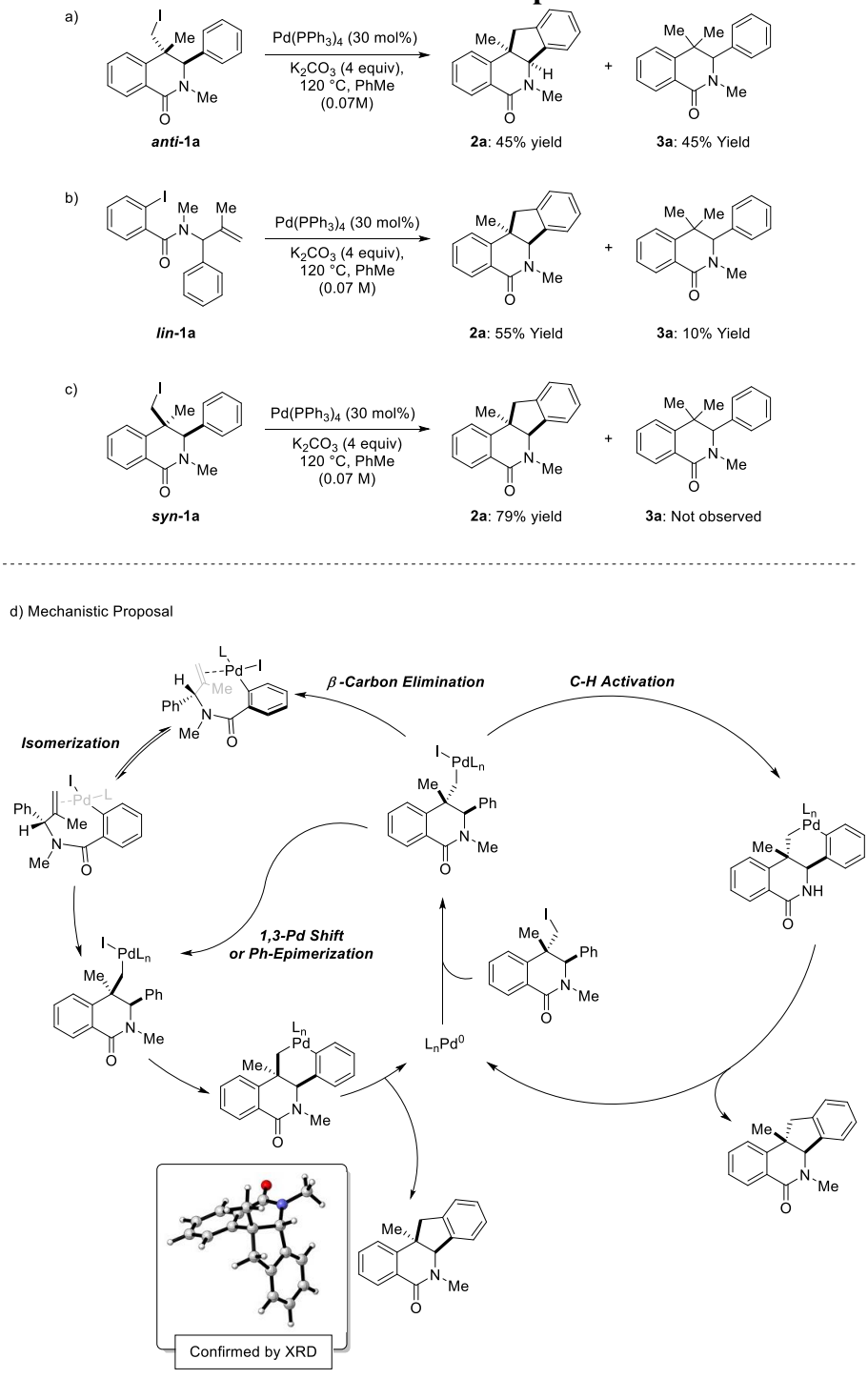

A series of experiments were designed to determine if a β-carbon elimination was the likely path. We hypothesized two alternative mechanisms could be operative in this process. The first involved a 1,3-palladium shift. Following oxidative addition to the neopentyl iodide, the palladium catalyst could undergo a C–H activation-protodemetallation sequence, forming the *syn* diastereomer. Subsequent C–H activation-reductive elimination would afford the product. Palladium-migrations

between two-carbons via a C–H activation have been reported in the literature,[48–50] and in these substrates, both would converge to the *syn*-neopentyl palladium species. A second mechanism leading to isomerization would occur via an epimerization at the other stereocenter containing the pendant aromatic ring. This epimerization would also allow for the generation of the *syn*-diastereomer, however it would lead to the enantiomeric product.

Scheme 3. Mechanistic Studies Probing Alternative Pathways

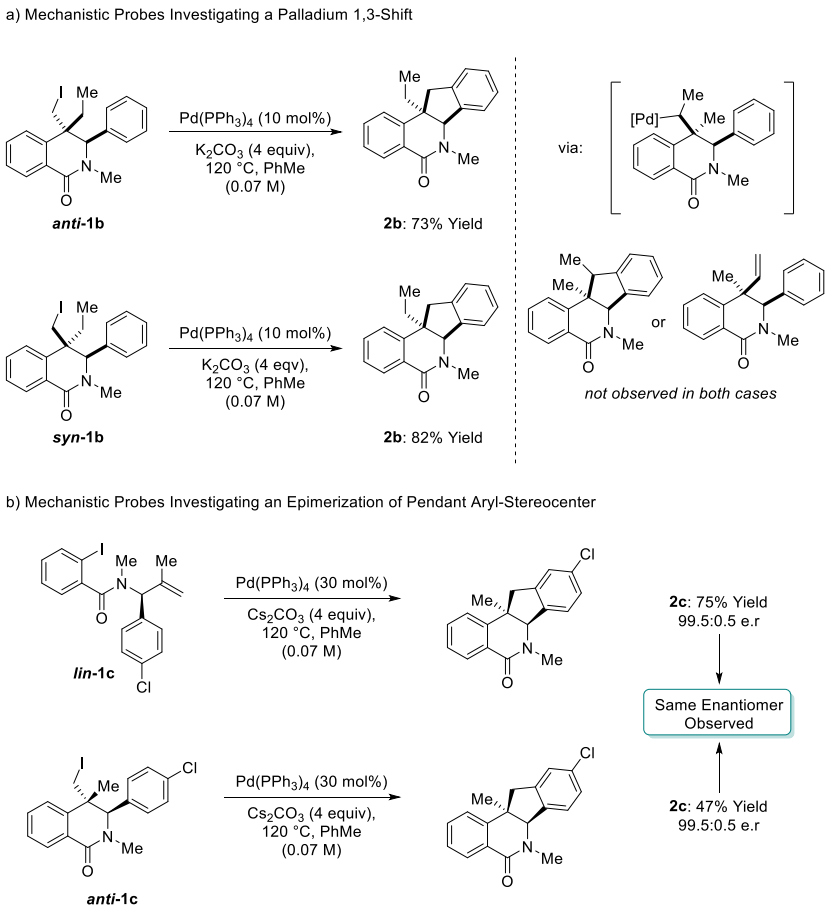

To probe the 1,3-palladium shift mechanism, we studied an analogous substrate bearing an ethyl group (Scheme 3a). We could envision 3 possible outcomes: an alkenyl derived product stemming from a 1,3-palladium shift and subsequent β-hydride elimination, a tetracyclic product bearing a methyl group where the previous diastereotopic methylenewould have been, or complete inhibition of the reaction. We observed the expected product of the β-carbon elimination cascade (**2b**) as the major product, in a yield of 73% from ***anti*-1b**, and 82% yield from ***syn*-1b**, using only 10 mol % catalyst, supporting that the reaction does not proceed via a 1,3-palladium shift.

To exclude the possibility of an aryl epimerization, we employed the enantioenriched starting material ***anti*-1c**, prepared from the corresponding aryl iodide ***lin*-1c** with the same absolute stereochemistry (Scheme 3b). If the *anti*-product was undergoing epimerization rather than retro-carbopalladation, we would have expected to isolate the enantiomer of the final product. Subjecting both substrates separately to the reaction conditions gave the identical enantiomer, **2c,** with no degradation in enantioselectivity. This result supports that stereocenter undergoing the epimerization was the quaternary all-carbon stereocenter.

We then turned to density functional theory (DFT) to study the energetic landscape of this reaction (Scheme 4a, see supporting information for computational details). We began our investigation from the palladium oxidative addition complex, **1**. Initial displacement of one of the PPh_3 ligands by the aromatic backbone provides intermediate **2**; subsequent β-carbon elimination (**TS 2-3**, $\Delta G^{\neq}$ = 35.7 kcal mol^{-1}) from this intermediate led to the formation of the olefin-coordinated palladium complex **3**. Notably, this process is endergonic by 26.5 kcal mol^{-1}, consistent with our hypothesis that this step does not have a thermodynamic driving force and should be reversible. Subsequent decoordination of the *si* face of the alkene from complex **3** followed by coordination of the *re* face of the alkene leads to aryl palladium complex, **4**. Migratory insertion of this complex (**TS 4-5**, $\Delta G^{\ddagger}$ = 8.3 kcal mol^{-1}) leads to the formation of the *syn* neopentyl palladium complex, **5**. It is interesting to highlight that palladium complex, **5**, is more stable than **1** ($\Delta G_{anti/syn}$ = -5.2 kcal mol^{-1}). Ligand exchange from **5** leads to the carbonate complex, **6**, which undergoes a C–H activation via an inner sphere concerted metalation deprotonation mechanism (**TS 6-7**, $\Delta G^{\ddagger}$ = 33.2 kcal mol^{-1}) to form palladacycle, **7**. Reductive elimination (**TS 7-8**, $\Delta G^{\ddagger}$ = 15.7 kcal mol^{-1}) leads to the formation of the *syn* indenodihydroisoquinolone and reforms the active palladium catalyst. The driving force for this process is the irreversible C–C bond reductive elimination (ΔG = -41.6 kcal mol^{-1}), which funnels complex **3** toward the desired product.

Scheme 4. Density Functional Theory (DFT) Analysis of the Reaction

a) DFT Analysis of Observed Reaction

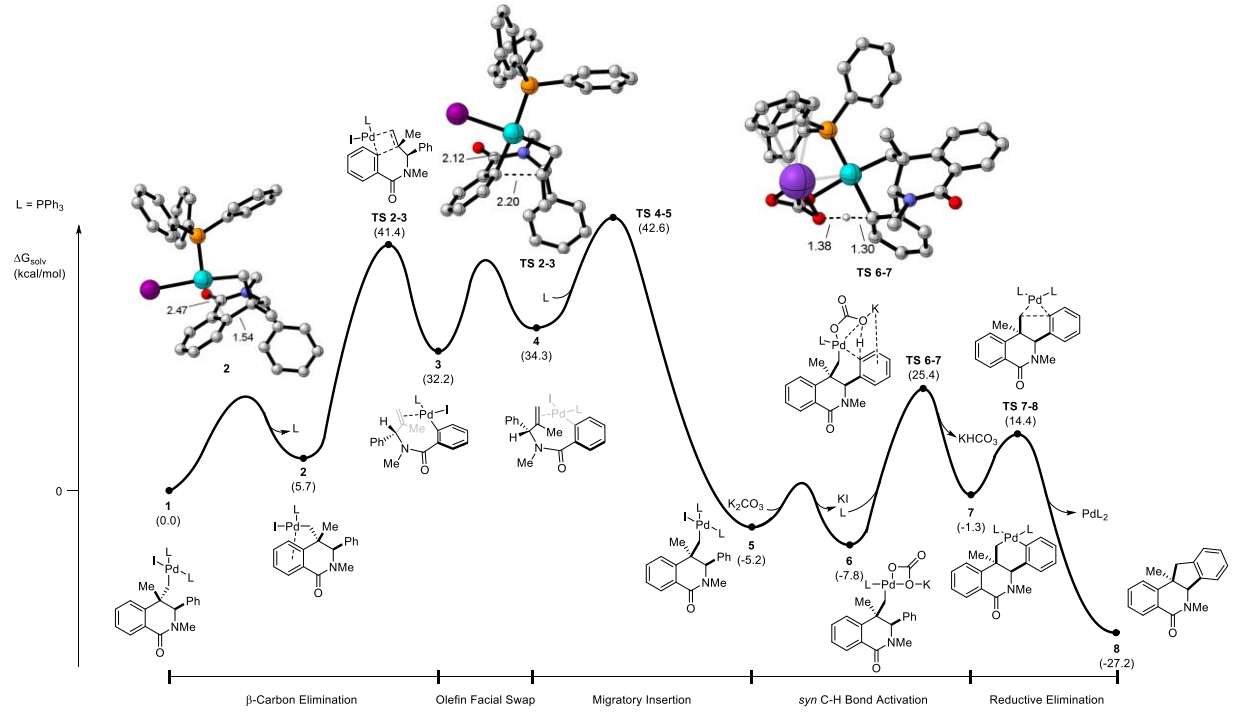

b) DFT Analysis of Unobserved anti-C–H Activation

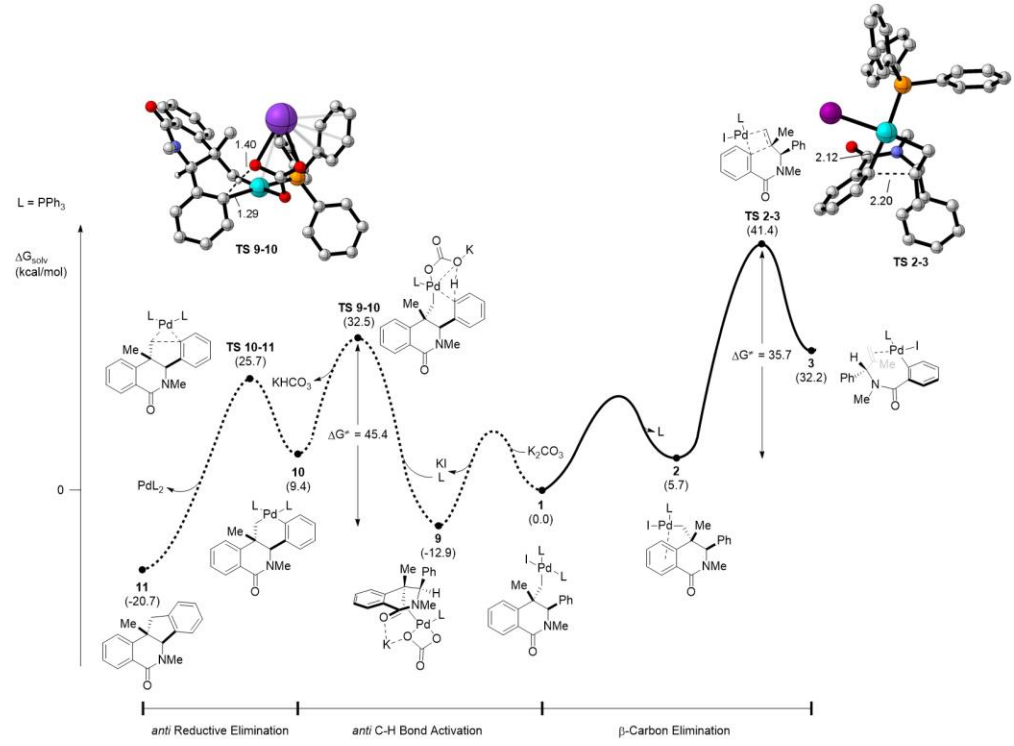

Although the *anti*-indenodihydroisoquinolone was never observed experimentally, we investigated the energetics of an *anti* C–H activation leading to this product (Scheme 4b). Formation of the carbonate complex, **9**, from **1** is exergonic by 12.9 kcal mol^{-1}. The C–H activation process leading to the *anti*-palladacycle, **10**, was computed to have an activation barrier of 45.4 kcal mol^{-1}. A comparison of the β-carbon elimination transition state, **TS 2-3**, with the *anti* C–H activation transition state, **TS 9-10**, reveals a $\Delta\Delta G^{\ddagger}$ = 9.7 kcal mol^{-1}, consistent with experimental observations.

The nickel-catalyzed carboiodination of **lin-1b** yielded a ~1:1 mixture of each of the diastereomers for the substrate bearing an ethyl group at the R^1 position. We set out to explore the opportunity to perform a unique convergence of the *syn*- and *anti*- diastereomers (Scheme 5a). By accessing the same catalytic cycle from different starting points, we were able to take a variety of *syn*- and *anti*-iodo-dihydroisoquinolones and selectively obtain the *syn*-indenodihydroisoquinolone product using 10 mol % of the palladium catalyst. Cs_2CO_3 was also found to give slightly better yields with these substrates. The presence of an ethyl group at the R^1 position generally gave better conversion than the methyl counterpart, with a significantly decreased amount of protodemetallation being observed. The substrate bearing an electron-deficient *p*-CF_3 group gave the product in 95% yield, as compared to the analogous substrate containing a methyl group which afforded the product in 58% yield using 30 mol % catalyst. Access to a key intermediate at a third point of the catalytic cycle was also achieved, namely from the linear aryl iodide starting material (Scheme 5b). When a 1:1:1 mixture of ***lin*-1b**, ***syn*-1b**, and ***anti*-1b** were subjected to the reaction conditions, the *syn*-indenoisoquinoline was obtained in 71% yield.

Scheme 5. Substrate Scope from Multiple Access Points

a) Diastereoconvergent Substrate Scope from 1:1 Mixture of Diastereomers

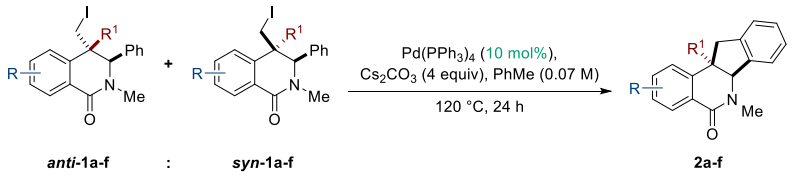

***anti*-1a-f** : ***syn*-1a-f** **2a-f**

Substrate Scope

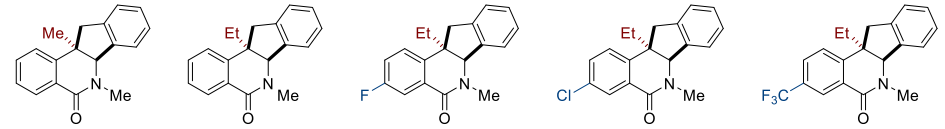

2a: 58% yield, > 20:1 d.r[a] | **2b**: 72% yield, > 20:1 d.r | **2d**: 74% yield, > 20:1 d.r | **2e**: 73% yield, > 20:1 d.r | **2f**: 95% yield, > 20:1 d.r

b) Triple Access-Point Experiment

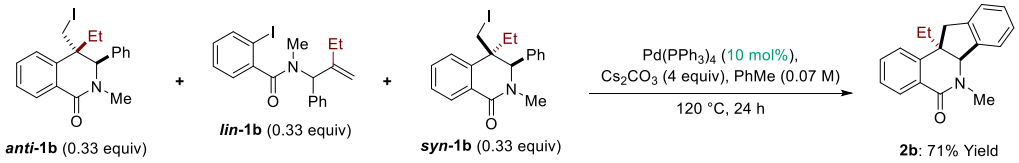

***anti*-1b** (0.33 equiv) + ***lin*-1b** (0.33 equiv) + ***syn*-1b** (0.33 equiv) → **2b**: 71% Yield

C) Effect of Stereoelectronics Parameters on the β-carbon Elimination

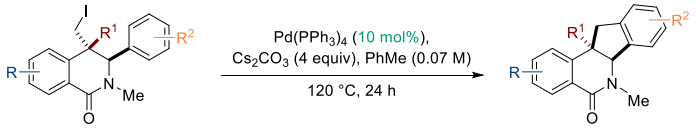

***anti*-1a-h** **2a-h**

Substrate Scope

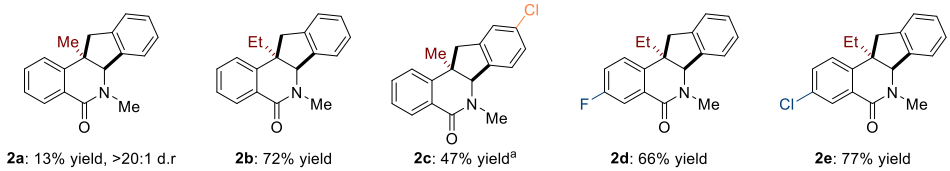

2a: 13% yield, >20:1 d.r
45% yield,> 20:1 d.r[a] | **2b**: 72% yield, > 20:1 d.r | **2c**: 47% yield[a]
>20:1 d.r, 99:1 e.r[b] | **2d**: 66% yield, > 20:1 d.r | **2e**: 77% yield, > 20:1 d.r

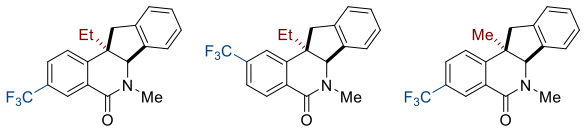

2f: 94% yield, > 20:1 d.r | **2g**: 86% yield, > 20:1 d.r | **2h**: 47% yield, > 20:1 d.r

a) Reaction was run with 30 mol% catalyst

Reactions using the *anti*-diastereomer typically gave slightly diminished yield when compared to the 1:1 mixture, which is likely due to the greater efficiency of the *syn*-isomer going to the product (Scheme 5c). Generally, electron-deficient substrates outperformed the electron-rich ones. The *p*- and *m*-CF_3 substrates gave the product in the highest yields (94% and 86% respectively). Even for substrates containing a methyl group at the R^1 position, incorporating a *p*-CF_3 group on the molecule resulted in full conversion of the starting material at only 10 mol % catalyst. The desired product was obtained in 47% yield and the remaining mass balance was the protodemetalation product. In comparison, the parent aryl substrate containing a methyl group gave 13% product and 58% of the protodemetalation with ~30% unreacted starting material at 10 mol % catalyst. Unfortunately, it was not possible to explore the reactivity of electron-rich substrates, as the nickel-carboiodination reaction failed to yield these parent compounds.

Given the impressive results with the *p*-CF_3 substrate described above, we hypothesized that the electron-withdrawing group may positively influence the β-carbon elimination process. Typically, the efficiency of β-carbon elimination is thought to be due to thermodynamic factors, such as relief of ring strain or extrusion of stable molecules such as a nitrile or carbonyl group, but the effect of electronic parameters is less understood. We examined the effect of *para* substitution on the β-carbon elimination using DFT (Scheme 6a). We found that the coordination of the aromatic ring to the palladium center was favoured when the substitution in the ring was electron-donating (ΔG = 4.8 kcal mol^{-1} when R = OMe and ΔG = 7.4 kcal mol^{-1} when R = CF_3). The inverse effect was observed in the β-carbon elimination transition state, where the electron-withdrawing CF_3 group lowered the activation barrier by 1.1 kcal mol^{-1} when compared to the unsubstituted substrate. We hypothesize the improved yields using these substrates arises because the rate of the reaction becomes faster than the off-cycle protodemetalation. Comparatively, the electron-donating OMe group raised the activation barrier by 0.8 kcal mol^{-1}. We hypothesize that the electron-withdrawing group may stabilize the build-up of partial negative charge on the *ipso* carbon in the transition state. Notably, the C–C bond distance in ***p*-OMe-TS 2-3** is 2.29 Å compared to 2.18 Å for ***p*-CF_3-TS 2-3** and 2.20 Å for **TS 2-3**, suggesting a later transition state when electron-donating groups are present on the aromatic backbone.

Scheme 6. DFT Analysis of the Electronic and Steric Trends of the Reaction

a) DFT Analysis of the Electronic Trend of the Reaction

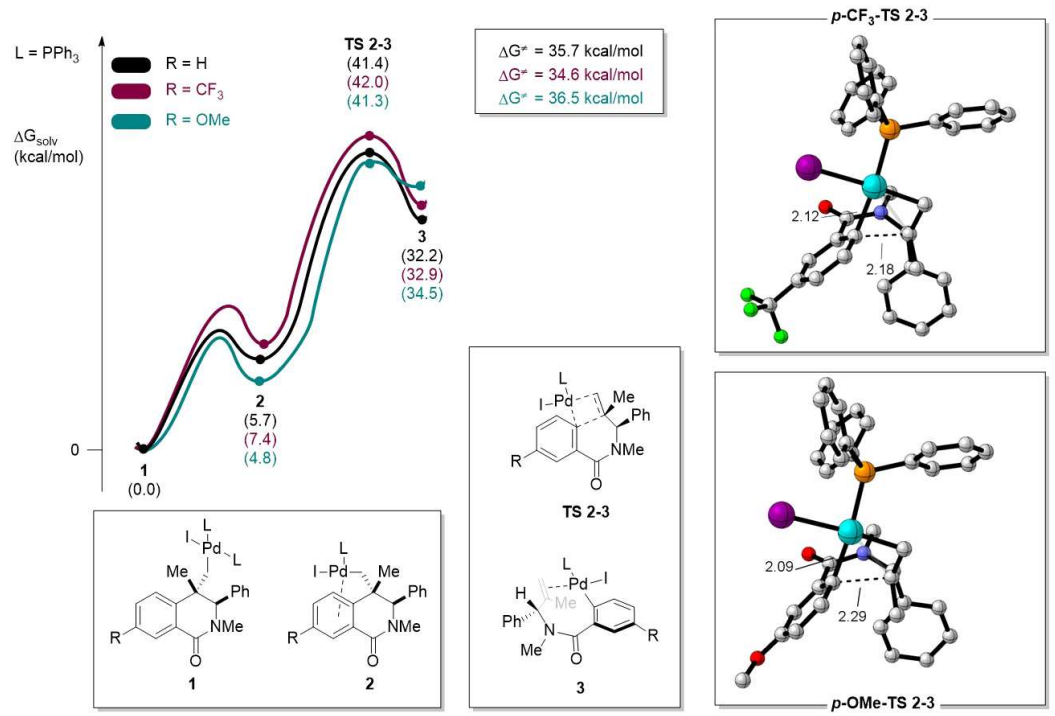

b) DFT Analysis of the Effect of the Ethyl group

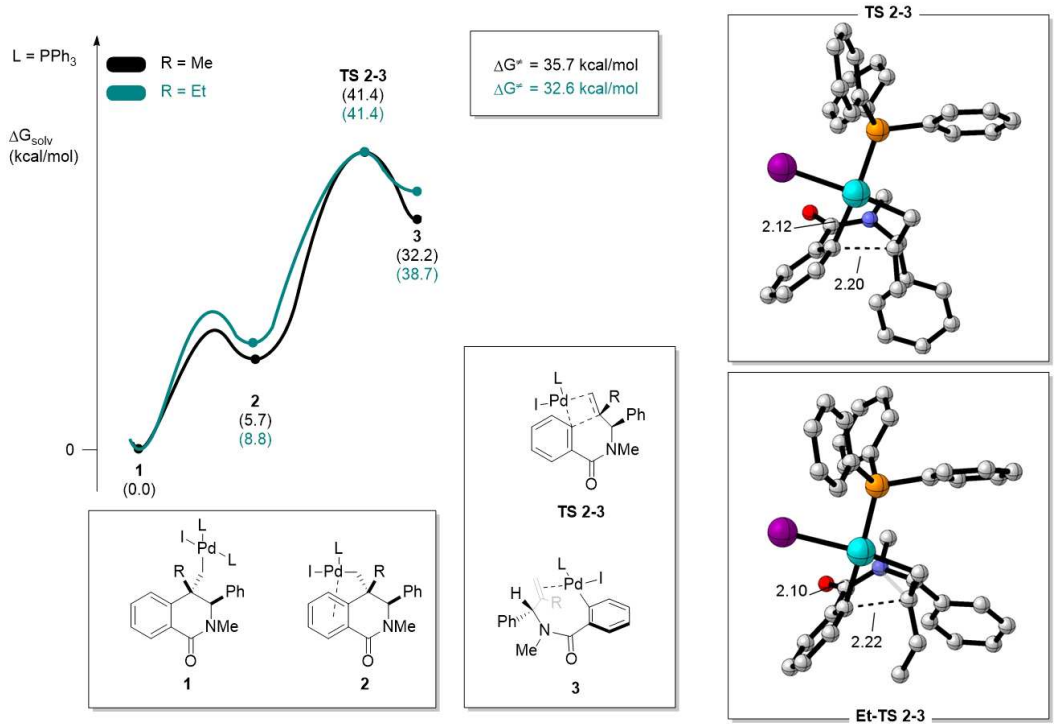

The origins behind the increased efficiency of substrates bearing an ethyl group at the R^1 position was investigated via DFT (Scheme 6b). It is possible the impact of the ethyl group arises through decreasing the barrier for the β-carbon elimination process by relieving increased steric strain. Alternatively, the intermediate palladium oxidative addition complex could have improved stability toward protodemetalation. Computational studies revealed that coordination of the aromatic ring to the palladium center required more energy for ethyl group system compared to that of the methyl (ΔG = 8.8 kcal mol^{-1} compared to ΔG = 5.7 kcal mol^{-1}). Interestingly, our analysis revealed that the activation energy for the β-carbon elimination transition state was lowered for R^1 = Et ($\Delta G^{\ddagger}$ = 32.6 kcal mol^{-1} for R = Et and $\Delta G^{\neq}$ = 35.7 kcal mol^{-1} for R = Me). Based on these results, we suggest that there is an increased level of steric build-up that is relieved upon β-carbon elimination when R = Et. We suspect that off-cycle pathways leading to protodemetalation are negligible due to this rate enhancement.

Conclusion

The use of nickel- and palladium-catalyzed carbohalogenation methodologies provided an ideal system on which to investigate metal catalyzed β-carbon elimination. From a synthetic perspective, mixtures of isomeric starting materials can be funneled into a single product bearing an all-carbon quaternary stereocenter through a diastereoconvergent process. Computational and experimental analyses revealed that the lifetime of the intermediate palladium oxidative addition complex, as well as the presence of electron-withdrawing groups, were instrumental in the success of the reaction. Identifying a mechanistic pathway that has not traditionally been accessible is the most interesting of the findings and opens the door to searching for other examples in diverse substrates and other catalysts.

Author Contributions

A.D.M and B.M contributed equally to this work. A.D.M and M.L conceived the idea for this work. A.D.M performed the experimental work for this the project, including the mechanistic studies, catalytic reactions, characterization and the majority of the substrate syntheses. B.M was responsible for all of the DFT calculations and aided in the design of the mechanistic studies and synthesis of the substrates. C.E.J aided in the synthesis of substrates and characterization. A.D.M, B.M and M.L prepared the manuscript with feedback from all the authors.

Acknowledgments

We thank the University of Toronto, the Natural Science and Engineering Research Council (NSERC), and Kennarshore Inc. for financial support. A.D.M. thanks NSERC for an NSERC Vanier fellowship. B.M. thanks the NSERC for a CGS D scholarship. Computational studies were enabled in part through support provided by Compute Ontario (www.computeontario.ca) and Compute Canada (www.computecanada.ca). We thank Dr. Darcy Burns, Dr. Jack Sheng and Dr. Karl Demmans (University of Toronto) for their assistance with NMR experiments. We thank Dr. Ivan Franzoni for his assistance with the DFT studies. We thank Dr. Alan Lough (University of Toronto) for obtaining the X-ray crystallographic data.

Data Availability

The authors declare that the data supporting the findings of this study are available in the manuscript and supplementary information.

References

1. Kotha, S. & Banerjee, S. Recent developments in the retro-Diels-Alder reaction. *RSC Adv.* **3**, 7642–7666 (2013).

2. Rickborn, B. The Retro–Diels–Alder Reaction Part II. Dienophiles with One or More Heteroatom. *Org. React.* **53**, 223–629 (2004).

3. Rickborn, B. The Retro-Diels-Alder Reaction. Part I. C-C Dienophiles. *Org. React.* **52**, 1–393 (2004).

4. Orlandi, M., Ceotto, M. & Benaglia, M. Kinetics versus thermodynamics in the proline catalyzed aldol reaction. *Chem. Sci.* **7**, 5421–5427 (2016).

5. Cergol, K. M., Jensen, P., Turner, P. & Coster, M. J. Reversibility in the boron-mediated ketone-ketone aldol reaction. *Chem. Commun.* 1363–1365 (2007) doi:10.1039/b617094c.

6. Zhang, J. *et al.* Kinetic Study of Retro-Aldol Condensation of Glucose to Glucolaldehyde With Ammonium Metatungstate as the Catalyst. *AIChE J.* **60**, 3804–2813 (2014).

7. Hartwig, J. F. *Organotransition metal chemistry: from bonding to catalysis*. (University Science Books, 2010).

8. Gómez-Gallego, M. & Sierra, M. A. Kinetic isotope effects in the study of organometallic reaction mechanisms. *Chem. Rev.* **111**, 4857–4963 (2011).

9. Blum, O. & Milstein, D. Mechanism of a Directly Observed β-Hydride Elimination Process of Iridium Alkoxo Complexes. *J. Am. Chem. Soc.* **117**, 4582–4594 (1995).

10. Vela, J. *et al.* Reversible beta-hydrogen elimination of three-coordinate iron(II) alkyl complexes: Mechanistic and thermodynamic studies. *Organometallics* **23**, 5226–5239 (2004).

11. Miura, M. & Satoh, T. Catalytic Processes Involving β-Carbon Elimination. *Top. Organomet. Chem.* **14**, 1–20 (2005).

12. Dong, G. *Topics in Current Chemistry: C-C Bond Activation*. vol. 346 (2014).

13. O'Reilly, M. E., Dutta, S. & Veige, A. S. β-Alkyl Elimination: Fundamental Principles and Some Applications. *Chem. Rev.* **116**, 8105–8145 (2016).

14. Ruhland, K. Transition-metal-mediated cleavage and activation of C-C single bonds. *European J. Org. Chem.* 2683–2706 (2012) doi:10.1002/ejoc.201101616.

15. Ye, J. *et al.* Remote C-H alkylation and C-C bond cleavage enabled by an in situ generated palladacycle. *Nat. Chem.* **9**, 361–368 (2017).

16. McDonald, T. R., Mills, L. R., West, M. S. & Rousseaux, S. A. L. Selective Carbon-Carbon Bond Cleavage of Cyclopropanols. *Chem. Rev.* **121**, 3–79 (2021).

17. Azizollahi, H. & García-López, J. A. Recent Advances on Synthetic Methodology Merging C-H Functionalization and C-C Cleavage. *Molecules* **25**, (2020).

18. Fumagalli, G., Stanton, S. & Bower, J. F. Recent Methodologies That Exploit C-C Single-Bond Cleavage of Strained Ring Systems by Transition Metal Complexes. *Chem. Rev.* **117**, 9404–9432 (2017).

19. Deng, R., Xi, J., Li, Q. & Gu, Z. Enantioselective Carbon-Carbon Bond Cleavage for Biaryl Atropisomers Synthesis. *Chem* **5**, 1834–1846 (2019).

20. Bunel, E., Burger, B. J. & Bercaw, J. E. Carbon-Carbon Bond Activation via /8-Alkyl Elimination. Reversible Branching of 1,4-Pentadienes Catalyzed by Scandocene Hydride Derivatives. *J. Am. Chem. Soc* **110**, 976–978 (1988).

21. Xia, Y. & Dong, G. Temporary or removable directing groups enable activation of unstrained C–C bonds. *Nat. Rev. Chem.* **4**, 600–614 (2020).

22. Cheng, H. G., Chen, S., Chen, R. & Zhou, Q. Palladium(II)-Initiated Catellani-Type Reactions. *Angew. Chem. Int. Ed.* **58**, 5832–5844 (2019).

23. Lutz, M. D. R. & Morandi, B. Metal-Catalyzed Carbon-Carbon Bond Cleavage of Unstrained Alcohols. *Chem. Rev.* **121**, 300–326 (2021).

24. Li, H. *et al.* Transformations of Aryl Ketones via Ligand-Promoted C−C Bond Activation. *Angew. Chem. Int. Ed.* **59**, 14388–14393 (2020).

25. Song, F., Gou, T., Wang, B. Q. & Shi, Z. J. Catalytic activations of unstrained C-C bond involving organometallic intermediates. *Chem. Soc. Rev.* **47**, 7078–7115 (2018).

26. Zheng, M. *et al.* Ligand-promoted alkynylation of aryl ketones: A practical tool for structural diversity in drugs and natural products. *ACS Catal.* 1758–1764 (2021) doi:10.1021/acscatal.0c05372.

27. Zhao, P. & Hartwig, J. F. β-aryl eliminations from Rh(I) iminyl complexes. *J. Am. Chem. Soc.* **127**, 11618–11619 (2005).

28. Zhao, P., Incarvito, C. D. & Hartwig, J. F. Direct observation of β-aryl eliminations from Rh(I) alkoxides. *J. Am. Chem. Soc.* **128**, 3124–3125 (2006).

29. Terao, Y., Wakui, H., Satoh, T., Miura, M. & Nomura, M. Palladium-catalyzed arylative carbon - Carbon bond cleavage of α,α-disubstituted arylmethanols [11]. *J. Am. Chem. Soc.* **123**, 10407–10408 (2001).

30. Newman, S. G. & Lautens, M. The role of reversible oxidative addition in selective palladium(0)- catalyzed intramolecular cross-couplings of polyhalogenated substrates:

Synthesis of brominated indoles. *J. Am. Chem. Soc.* **132**, 11416–11417 (2010).

31. Marchese, A. D., Larin, E. M., Mirabi, B. & Lautens, M. Metal-Catalyzed Approaches toward the Oxindole Core. *Acc. Chem. Res.* **53**, 1605–1619 (2020).

32. Jones, D. J., Lautens, M. & McGlacken, G. P. The emergence of Pd-mediated reversible oxidative addition in cross coupling, carbohalogenation and carbonylation reactions. *Nat. Catal.* **2**, 843–851 (2019).

33. Newman, S. G. & Lautens, M. Palladium-catalyzed carboiodination of alkenes: Carbon-carbon bond formation with retention of reactive functionality. *J. Am. Chem. Soc.* **133**, 1778–1780 (2011).

34. Liu, H., Li, C., Qiu, D. & Tong, X. Palladium-catalyzed cycloisomerizations of (Z)-1-iodo-1,6-dienes: Iodine atom transfer and mechanistic insight to alkyl iodide reductive elimination. *J. Am. Chem. Soc.* **133**, 6187–6193 (2011).

35. Zhang, Z. M. *et al.* Palladium/XuPhos-Catalyzed Enantioselective Carboiodination of Olefin-Tethered Aryl Iodides. *J. Am. Chem. Soc.* **141**, 8110–8115 (2019).

36. Sun, Y. L. *et al.* Enantioselective Cross-Exchange between C−I and C−C σ Bonds. *Angew. Chem. Int. Ed.* **58**, 6747–6751 (2019).

37. Petrone, D. A., Yoon, H., Weinstabl, H. & Lautens, M. Additive effects in the palladium-catalyzed carboiodination of chiral N-allyl carboxamides. *Angew. Chem. Int. Ed.* **53**, 7908–7912 (2014).

38. Yoon, H., Marchese, A. D. & Lautens, M. Carboiodination Catalyzed by Nickel. *J. Am. Chem. Soc.* **140**, 10950–10954 (2018).

39. Takahashi, T. *et al.* Nickel-catalyzed intermolecular carboiodination of alkynes with aryl iodides. *Chem. Commun.* **54**, 12750–12753 (2018).

40. Marchese, A. D., Lind, F., Mahon, Á. E., Yoon, H. & Lautens, M. Forming Benzylic Iodides via a Nickel Catalyzed Diastereoselective Dearomative Carboiodination Reaction of Indoles. *Angew. Chem. Int. Ed.* **58**, 5095–5099 (2019).

41. Marchese, A. D., Kersting, L. & Lautens, M. Diastereoselective nickel-catalyzed carboiodination generating six-membered nitrogen-based heterocycles. *Org. Lett.* **21**, 7163–7168 (2019).

42. Marchese, A. D. *et al.* Nickel-Catalyzed Enantioselective Carbamoyl Iodination: A Surrogate for Carbamoyl Iodides. *ACS Catal.* **10**, 4780–4785 (2020).

43. Marchese, A. D., Adrianov, T., Köllen, M. F., Mirabi, B. & Lautens, M. Synthesis of Carbocyclic Compounds via a Nickel-Catalyzed Carboiodination Reaction. *ACS Catal.* **11**, 925–931 (2021).

44. Marchese, A. D., Adrianov, T. & Lautens, M. Recent Strategies for Carbon-Halogen Bond Formation Using Nickel. *Angew. Chem. Int. Ed.* 2–15 (2021) doi:10.1002/anie.202101324.

45. Lan, Y., Liu, P., Newman, S. G., Lautens, M. & Houk, K. N. Theoretical study of Pd(0)-catalyzed carbohalogenation of alkenes: Mechanism and origins of reactivities and selectivities in alkyl halide reductive elimination from Pd(ii) species. *Chem. Sci.* **3**, 1987–1995 (2012).

46. Yoon, H., Petrone, D. A. & Lautens, M. Diastereoselective palladium-catalyzed arylcyanation/heteroarylcyanation of enantioenriched N -allylcarboxamides. *Org. Lett.* **16**, 6420–6423 (2014).

47. Jayanth, T. T., Zhang, L., Johnson, T. S. & Malinakova, H. C. Sequential Cu(I)/Pd(0)-catalyzed multicomponent coupling and annulation Protocol for the synthesis of indenoisoquinolines. *Org. Lett.* **11**, 815–818 (2009).

48. Huang, Q., Fazio, A., Dai, G., Campo, M. A. & Larock, R. C. Pd-catalyzed alkyl to aryl migration and cyclization: An efficient synthesis of fused polycycles via multiple C-H activation. *J. Am. Chem. Soc.* **126**, 7460–7461 (2004).

49. Piou, T., Bunescu, A., Wang, Q., Neuville, L. & Zhu, J. Palladium-catalyzed through-space C(sp3)-H and C(sp 2)-H bond activation by 1,4-palladium migration: Efficient synthesis of [3,4]-fused oxindoles. *Angew. Chem. Int. Ed.* **52**, 12385–12389 (2013).

50. Clemenceau, A., Thesmar, P., Gicquel, M., Le Flohic, A. & Baudoin, O. Direct Synthesis of Cyclopropanes from gem-Dialkyl Groups through Double C-H Activation. *J. Am. Chem. Soc.* **142**, 15355–15361 (2020).

Supplementary Files

This is a list of supplementary files associated with this preprint. Click to download.

- SupportingInformationReversibleCXXXCBondFormationUsingPalladiumCatalysis.pdf